Quantum Thermodynamics of Holographic Quenches and Bounds on the Growth of Entanglement from the Quantum Null Energy Condition

Tanay Kibe,* Ayan Mukhopadhyay,† and Pratik Roy‡
Center for Quantum Information Theory of Matter and Spacetime, and Center for Strings, Gravitation and Cosmology, Department of Physics, Indian Institute of Technology Madras, Chennai 600036, India

(Received 27 September 2021; revised 20 March 2022; accepted 21 April 2022; published 9 May 2022)

The quantum null energy condition (QNEC) is a lower bound on the energy-momentum tensor in terms of the variation of the entanglement entropy of a subregion along a null direction. To gain insights into quantum thermodynamics of many-body systems, we study if the QNEC restricts irreversible entropy production in quenches driven by energy-momentum inflow from an infinite memoryless bath in two-dimensional holographic theories. We find that an increase in both entropy and temperature, as implied by the Clausius inequality of classical thermodynamics, is necessary but not sufficient to not violate QNEC in quenches leading to transitions between thermal states with momentums that are dual to Banados-Teitelboim-Zanelli geometries. For an arbitrary initial state, we can determine the lower and upper bounds on the increase of entropy (temperature) for a fixed increase in temperature (entropy). Our results provide explicit instances of quantum lower and upper bounds on irreversible entropy production whose existence has been established in literature. We also find monotonic behavior of the nonsaturation of the QNEC with time after a quench, and analytically determine their asymptotic values. Our study shows that the entanglement entropy of an interval of length l always thermalizes in time $l/2$ with an exponent $3/2$. Furthermore, we determine the coefficient of initial quadratic growth of entanglement analytically for any l, and show that the slope of the asymptotic ballistic growth of entanglement for a semi-infinite interval is twice the difference of the entropy densities of the final and initial states. We determine explicit upper and lower bounds on these rates of growth of entanglement.

DOI: 10.1103/PhysRevLett.128.191602

Quantum thermodynamics has established various instances where thermodynamics can be generalized even to finite-dimensional quantum systems interacting with a bath by accounting for entanglement and measures of accessible quantum information [1–7]. For instance, it has been shown that the one-shot work cost of creating a state and the extractable work from it are bounded by the hypothesis-testing relative entropy between the state and the thermal equilibrium [3]. This discipline has found applications in understanding (bio-)chemical reactions, and also in the study of quantum engines.

Although limited progress has been achieved in the applications of quantum thermodynamics to many-body systems, there have been independent developments of interest. One such example is the formulation of the quantum null energy condition (QNEC) [8], which sets lower bounds on the expectation value of null components of the energy-momentum tensor in terms of null variations of the entanglement entropy of subregions whose boundary contains the point of observation. QNEC has been proven for free quantum field theories (QFTs) [9,10], holographic QFTs [11], two-dimensional (2D) conformal field theories (CFTs) [12], and also for general Poincaré-invariant QFTs using half-sided modular inclusion properties of operator algebras [13]. In a 2D CFT with central charge c, the strictest form of QNEC is [11,12,14]

$$\mathcal{Q}_{\pm} \equiv 2\pi\langle t_{\pm\pm}\rangle - S''_{\mathrm{ent}} - \frac{6}{c}S'^{2}_{\mathrm{ent}} \geq 0, \tag{1}$$

where $t_{\pm\pm}$ are the two nonvanishing null components of the energy-momentum tensor, and the derivatives are obtained from infinitesimal variations of the entanglement entropy S_{ent} of any interval ending at the point of observation under shifts along the $+$ (right) and $-$ (left) pointing null directions, respectively. Recently it has been pointed out that QNEC can follow from positivity conditions on variations of the relative entropy under null shape deformations [15–17] (see also Ref. [13]) and such positivity conditions also hold for sandwiched Renyi divergences. A pertinent question is therefore, whether QNEC and its possible generalizations impose criteria that go beyond classical thermodynamics,

such as quantum generalizations of the Clausius inequality discussed in the literature [18–23].

When any system with finite energy interacts with a memoryless infinitely large energy bath, its entropy can only increase monotonically. In holographic QFTs, this feature is reproduced via the monotonic growth of the area of the apparent and event horizons, and eventual thermalization following a quench [24–27].

In this Letter, we consider fast quenches that lead to transitions between thermal states carrying momentum in 2D holographic systems, and establish that the QNEC implies more than the mere rise of both the temperature and the thermodynamic entropy. For a fixed increase in the entropy (temperature), the increase in temperature (entropy) has to be bounded from both above and below so that the QNEC is unviolated after quench. Our results thus provide explicit instances of the upper and lower bounds on irreversible entropy production in quantum many-body systems whose existence has been established using tools of quantum information theory [18–23]. Furthermore, we extend previous results [28–36] on the growth and thermalization of entanglement entropy in 2D CFTs, and establish bounds on the rates of growth of entanglement that can be validated in numerical simulations and experiments.

Our holographic results apply when the central charge c of the CFT is large and it has a sparse spectrum (implying strong coupling). Nevertheless, we argue that our results are relevant for understanding entropy production from quenches faster than any microscopic timescale in a generic many-body system.

Holographic quenches.—A two-dimensional strongly coupled holographic CFT with a large central charge can be described by a three-dimensional Einstein gravity coupled to a few fields and with a negative cosmological constant [37]. The central charge of the dual CFT is $c = 3L/(2G)$ [38–40], where G is Newton's gravitational constant and L is related to the cosmological constant Λ via $\Lambda = -1/L^2$. Any (time-dependent) state in the CFT corresponds to a regular solution of the gravitational theory.

Quenches leading to fast transitions between thermal states at time $t = 0$ can be described by dual metrics of the form (see also Ref. [41])

$$ds^2 = 2drdt - \left(\frac{r^2}{L^2} - 2m(t)L^2\right)dt^2 + 2j(t)L^2 dtdx + \frac{r^2}{L^2}dx^2, \tag{2}$$

with

$$m(t) = \theta(-t)(\mu_+^{i2} + \mu_-^{i2}) + \theta(t)(\mu_+^{f2} + \mu_-^{f2}), \tag{3}$$

$$j(t) = \theta(-t)(\mu_+^{i2} - \mu_-^{i2}) + \theta(t)(\mu_+^{f2} - \mu_-^{f2}), \tag{4}$$

where $\mu_\pm^{i,f}$ are related to the temperature ($T^{i,f}$) and entropy density ($s^{i,f}$) of the initial and final thermal states respectively. Explicitly,

$$T^{i,f} = \frac{2}{\pi}\frac{\mu_+^{i,f}\mu_-^{i,f}}{\mu_+^{i,f} + \mu_-^{i,f}}, \qquad s^{i,f} = \frac{c}{6}(\mu_+^{i,f} + \mu_-^{i,f}). \tag{5}$$

These can be obtained from the thermodynamics of the Banados-Teitelboim-Zanelli (BTZ) black branes [42,43] dual to the initial and final states. The coordinates t and x are shared by the dual field theory that lives at the boundary $r = \infty$ of the emergent radial direction. This geometry is supported by a bulk stress tensor T_{MN} that is traceless and locally conserved in the metric [Eq. (2)] with nonvanishing components

$$T_{tt} = \frac{q(t)L^2}{r} + \frac{p(t)j(t)L^6}{r^3}, \qquad T_{tx} = \frac{p(t)L^2}{r}, \tag{6}$$

where

$$\begin{aligned} 8\pi G q(t) &= \delta(t)(\mu_+^{f2} - \mu_+^{i2} + \mu_-^{f2} - \mu_-^{i2}), \\ 8\pi G p(t) &= \delta(t)(\mu_+^{f2} - \mu_+^{i2} - \mu_-^{f2} + \mu_-^{i2}). \end{aligned} \tag{7}$$

We find that the QNEC inequalities [Eq. (1)] imply that the bulk matter satisfies the classical null energy condition.

Holographic renormalization [39,40] of the on-shell gravitational action for the metric [Eq. (2)] provides the expectation value of the energy-momentum tensor of the dual state (living in flat Minkowski metric):

$$\langle t_{\pm\pm}\rangle = \frac{c}{12\pi}(\theta(-t)\mu_\pm^{i2} + \theta(t)\mu_\pm^{f2}), \qquad \langle t_{+-}\rangle = 0. \tag{8}$$

The vanishing of $\langle t_{+-}\rangle$ implies tracelessness. Gravitational constraints [Eq. (7)] also imply the Ward identity $\partial_\mu\langle t^{\mu\nu}\rangle = f^\nu$, where $f_\nu = L[q(t,x), p(t,x)]$ is the energy-momentum injection from the infinite bath into the CFT.

Finally, we note that we have been agnostic about the matter content of the bulk theory while describing the dual geometries. The explicit form [Eq. (7)] of the bulk energy-momentum tensor, which is localized on the ingoing null shell, is simply necessitated by the Israel junction conditions. Our results therefore do not depend on the specific details of the dual CFTs.

For our analytic computations, we use the result that the geometry [Eq. (2)] describing a fast transition between two BTZ black branes at $t = 0$ can be *uniformized*, i.e., converted to the Poincaré patch metric [with $m(t) = j(t) = 0$ in Eq. (2)], corresponding to the vacuum, with two *separate* diffeomorphisms for $t < 0$ and $t > 0$ (see the Supplemental Material [44] for details). These uniformization maps result in two Poincaré patches bounded by the hypersurfaces $[\Sigma^{i,f}(x,r)]$ that are the respective images of the hypersurface

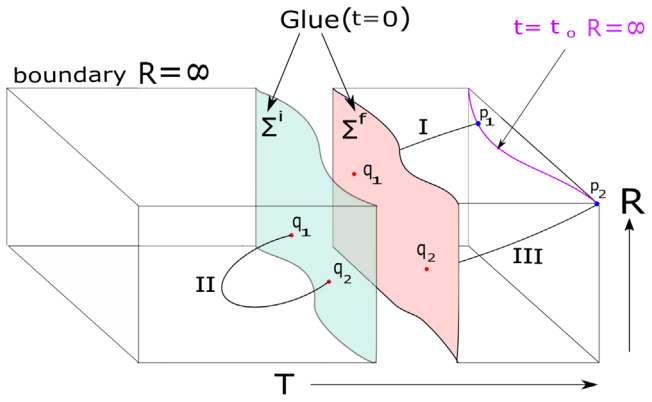

FIG. 1. Schematic representation of the cut and glue method—the left and right halves represent the separate Poincaré patches to which the prequench and postquench spacetimes map to. The gluing hypersurfaces $\Sigma^{i,f}$ are the images of $t = 0$ in the respective geometries. Points on $\Sigma^{i,f}$ carrying the same physical coordinate labels x and r are identified. The geodesic ending at the boundary is cut into three arcs.

$t = 0$. These hypersurfaces are glued by identifying the points on each with the same values of the *physical* coordinates x and r. See Fig. 1 for an illustration.

Entanglement growth.—The entanglement entropy of a spacelike interval with end points $p_1 = (x_1, t_1)$ and $p_2 = (x_2, t_2)$ in any arbitrary state of the holographic CFT can be obtained from the proper length L_{geo} of the geodesic in the dual bulk geometry that is anchored to the points p_1 and p_2 at the regulated boundary $r = L^2/\epsilon$, and is given by $S_{\text{ent}} = (c/6)(L_{\text{geo}}/L)$ [48,49]. Here, ϵ^{-1} is interpreted as an ultraviolet energy cutoff in the dual theory. Since the geodesic length can be readily computed in the Poincaré patch metric given just the endpoints [50], we can compute the entanglement entropy of a spatial interval of length l in any BTZ state employing the uniformization map. A simple computation yields

$$S_{\text{ent}} = \frac{c}{6}\ln\left[\frac{\sinh(\mu_+ l)\sinh(\mu_- l)}{\mu_+\mu_- l^2}\right] + \frac{c}{3}\ln\left(\frac{l}{\epsilon}\right), \tag{9}$$

where the last term is the well-known vacuum contribution that depends on the ultraviolet regulator (see Refs. [28,51,52]).

Via the cut and glue method we can readily compute the evolution of entanglement entropy for intervals at the boundary of geometries describing fast quenches between two BTZ spacetimes. Before the quench, the geodesic is located entirely in a single Poincaré patch described by the uniformization map for $t < 0$. After the quench, the geodesic anchored to the boundary (at points $p_{1,2}$ in Fig. 1) of the final Poincaré patch goes back in time and intersects the gluing hypersurface Σ^f, at two points ($q_{1,2}$ in Fig. 1) until a limiting time where the two intersection points merge, after which the entanglement entropy for the chosen interval thermalizes. The hypersurface Σ^f thus cuts the geodesic into three arcs, two of which (labeled I and III in Fig. 1) are in the final Poincaré patch and join $p_{1,2}$ to $q_{1,2}$ on Σ^f, and a third arc (labeled II in Fig. 1) joins $q_{1,2}$ on Σ^i in the initial Poincaré patch. The length of each of the three geodetic arcs can be computed by the Poincaré patch distance formula since the endpoints are known explicitly. Variations of the entanglement entropy under null deformations of any of the endpoints can similarly be computed. For more details, see the Supplemental Material [44].

Our explicit computations confirm that the entanglement entropy has three stages of evolution [31–33] for a transition between two BTZ spacetimes. In the first stage, the entanglement entropy of an interval of length l grows quadratically from its prequench values as $\sim D_s t^2$ with

$$D_s = \frac{c}{6}\{\Delta m + 2[\mu_+^f \coth(\mu_+^f l) - \mu_+^i \coth(\mu_+^i l)] \times [\mu_-^f \coth(\mu_-^f l) - \mu_-^i \coth(\mu_-^i l)]\}, \tag{10}$$

where $\Delta m = \mu_+^{f2} + \mu_-^{f2} - \mu_+^{i2} - \mu_-^{i2}$. The above reproduces the known result for the vacuum to thermal nonrotating BTZ transition [31,33]. This initial quadratic growth has also been observed in quantum lattice systems [53,54]. In the intermediate regime, the entanglement grows quasilinearly. For a semi-infinite interval, the asymptotic growth is exactly linear, i.e., $S_{\text{ent}} = v_s t$ with

$$v_s = 2(s^f - s^i), \tag{11}$$

where $s^{i,f}$ are the initial (final) entropy densities given by Eq. (5). This is consistent with the "tsunami hypothesis" [32,36] (see also Refs. [55–57]) that the entanglement *spreads* with a tsunami velocity, which is the speed of light in 2D CFTs [30,36], from both ends of the interval so that subintervals of total length $2t$ should become completely entangled with the rest of the quenched system. If an interval of large length can be approximated by a thermal density matrix (see Refs. [30,58–60]), then the result [Eq. (11)] follows because the change in the entanglement at late time should be the product of the length $2t$ times the difference in the thermodynamic entropy densities between final and initial states (see Refs. [61,62] for other contexts). This light-cone-like spreading of entanglement has been observed analytically in CFTs using replica methods [29], numerically in quantum lattice systems [63–67], and experimentally in ultracold atomic gases [68,69] and ion traps [70–72]. Our general result [Eq. (11)] can thus be validated both numerically and experimentally.

We are also able to prove that the entanglement entropy $S^{\text{ent}}(t)$ for any interval of length l saturates sharply to the thermal value S_{th} at the so-called "horizon time" $t = l/2$ and also seen in lattice simulations as $S_{\text{th}} - S^{\text{ent}}(t) \sim (l/2 - t)^{3/2}$ as $t \to l/2$ for arbitrary fast quenches. This readily follows from the analytic result that the final intersection point

between Σ^f and the geodesic glued to the endpoints of the interval $0 \le x \le l$ at the boundary in the postquench geometry occurs at $t = l/2$, and is given by the point on Σ_f parametrized by

$$r_* = L^2[\mu_+^f \coth(\mu_+^f l) + \mu_-^f \coth(\mu_-^f l)], \qquad x_* = l/2. \quad (12)$$

The horizon time and the saturation exponent $3/2$ were found earlier in holographic systems only for the transition from the vacuum to a nonrotating thermal state [31–33]. However, this feature can be shown to be valid analytically for a class of quenches in generic 2D CFTs [29,30,36] and is also seen in experiments [68]. It will be interesting to also reproduce our general results from tensor network approaches building on [73].

The QNEC criterion.—It can be readily seen that the momentum carrying thermal states dual to BTZ geometries saturate the QNEC inequalities [Eq. (1)] for any length l of the entangling interval [74]. Therefore, these inequalities should be saturated before the quench. However, after the quench time ($t = 0$), we find that the QNEC inequalities [Eq. (1)] can be violated.

We find that the QNEC inequalities [Eq. (1)] imply the strictest bounds when applied for the semi-infinite interval (see the Supplemental Material [44] for dependence of $\mathcal{Q}_\pm(t)$ on the length l of the entangling interval). Translation symmetry further implies that it is sufficient to consider intervals $x \ge 0$ with $\mathcal{Q}_+$ ($\mathcal{Q}_-$) involving null variations of the endpoint at the spatial origin towards right (left), respectively. Applying the cut and glue method for the semi-infinite interval, we see that demanding $\mathcal{Q}_\pm \ge 0$ at $t = 0$ implies [with $\Delta = 2(\mu_+^f - \mu_+^i)(2\mu_+^f + \mu_+^i)$]:

$$\frac{1}{3}\left(\sqrt{\Delta + 3\mu_-^i(3\mu_-^i + 2\mu_+^i - 2\mu_+^f)} + \mu_+^f - \mu_+^i\right)$$
$$\le \mu_-^f \le \sqrt{\Delta + \mu_-^i(\mu_-^i + 2\mu_+^f - 2\mu_+^i)} - \mu_+^f + \mu_+^i. \quad (13)$$

For the initial vacuum state ($\mu_\pm^i = 0$), the above inequalities simply impose that $\mu_+^f = \mu_-^f$, i.e., the final state should have zero momentum. One can analytically show that for the latter case $\mathcal{Q}_\pm = 0$ for all time in the case of the semi-infinite interval (see the Supplemental Material [44]). It is quite interesting that although the thermalization of the entanglement occurs at the tsunami speed (of light), QNEC saturation persists throughout the quench.

When the initial state is not the vacuum, the inequality [Eq. (13)] implies that $\mu_\pm^f \ge \mu_\pm^i$, and therefore $T^f > T^i$ and $s^f > s^i$, i.e., both the temperature and thermodynamic entropy density must not decrease after quench. However, as stated before, we get more. As for instance, with $\mu_+^i = 1$, $\mu_-^i = 0.75$ the final states satisfying Eq. (13) lie within the region bounded by the black bold lines shown at the left in Fig. 2, implying stricter bounds than classical thermodynamics. When the upper (lower) end of the inequality

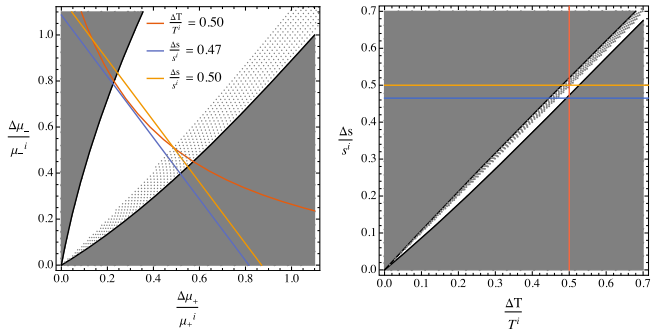

FIG. 2. Left: The possible relative changes $[(\mu_\pm^f - \mu_\pm^i)/\mu_\pm^i]$ for $\mu_+^i = 1$, $\mu_-^i = 0.75$ are shown in white. The black lines are given by the inequality [Eq. (13)] required by $\mathcal{Q}_\pm \ge 0$ at $t = 0$ and the gray dotted region is disallowed by examining $\mathcal{Q}_-$ for $t > 0$. The contours show that for a fixed change in temperature (red), the change in entropy is bounded from above and below (yellow and blue). Right: The same allowed region (in white) is shown in terms of the relative change in temperature and entropy density.

[Eq. (13)] is satisfied, $\mathcal{Q}_+$ ($\mathcal{Q}_-$) vanishes at $t = 0$ for the semi-infinite interval. For $t > 0$, although $\mathcal{Q}_+ > 0$ is always satisfied when Eq. (13) holds, $\mathcal{Q}_- \ge 0$ is violated for $t > t_c$ (with t_c depending on initial and final states), thus pushing above the lower bound on μ_-^f set by Eq. (13), depicted by the upper boundaries of the dotted regions in Fig. 2 (see the Supplemental Material [44] for more details). The final allowed region, shown in white in Fig. 2, implies lower and upper bounds on the increase in entropy density (temperature) for a fixed increase in temperature (entropy density). The corresponding plot of allowed final states for the initial state $\mu_\pm^i = 1$ shown in the Supplemental Material [44] also illustrates these bounds.

Furthermore, we find that, as $t \to \infty$,

$$\mathcal{Q}_- \to 0, \qquad \mathcal{Q}_+ \to (s^f - s^i)(\mu_+^f - \mu_-^f + \mu_+^i + \mu_-^i) > 0 \quad (14)$$

for the semi-infinite interval. Interestingly, for allowed transitions, $\mathcal{Q}_+(t)$ and $\mathcal{Q}_-(t)$ for the semi-infinite interval are also monotonically increasing and decreasing functions, respectively, after quench. Its implications for the relative entropy of the quenched state should be understood following [16,75] (see also Refs. [15,17]).

The bounds shown in Fig. 2 can be understood in terms of irreversible entropy production. For any process the total change in entropy can be decomposed as $\Delta S = \Delta S_{\rm irr} + \Delta S_{\rm rev}$, where $\Delta S_{\rm rev}$ is the entropy change due to reversible heat exchange with a bath. The Clausius inequality implies that $\Delta S_{\rm irr} \ge 0$. This has been generalized in quantum thermodynamics. Reference [18] provides a lower bound on $\Delta S_{\rm irr}$ in terms of the Bures distance between the out-of-equilibrium state and the final equilibrium state, and an upper bound related to the Bremermann-Bekenstein bound [76]. These bounds can be equivalently stated in terms of the average irreversible work [19–21]. Bounds on $\Delta S_{\rm irr}$ have

also been seen for an open quantum system coupled to a thermal bath [19,22,23]. However, such bounds depend on the choice of a distance measure on the space of states, and it is not clear which one places the tightest bound. The fast quenches considered here do not involve any reversible heat exchange, implying $\Delta S = \Delta S_{\rm irr}$. Our results provide an explicit computation of lower and upper bounds on $\Delta S_{\rm irr}$ for a fixed change in temperature in a strongly interacting many-body system.

The upper and lower bounds on Δs, the increase in entropy density, for a fixed final temperature and a given initial state, readily bound the speed of the asymptotic ballistic entanglement growth [Eq. (11)] for the semi-infinite interval from both above and below. Furthermore, the coefficient of the initial quadratic growth [Eq. (10)] is similarly bounded from above and below for any l, and both of these bounds increase monotonically with l (see the Supplemental Material [44] for plots).

Our results should be valid when the timescale of the quench is smaller than any other scale in the system, and the final and initial temperature scales are both smaller than the microscopic energy scale below which the CFT provides a good description [36,77]. Since the strongest bounds on irreversible entropy production and entanglement growth correspond to the semi-infinite interval, our results are insensitive to the microscopic details. Our bounds can thus be verified qualitatively from growth of entanglement by studying fast quenches, e.g., in spin-$\frac{1}{2}$ XX and XXZ chains numerically [53,54], and experimentally in ultracold atomic gases [68,69] and in ion traps [70–72]. Going beyond the requirements $c \gg 1$ and a sparse spectrum would require investigating higher derivative and quantum corrections in the gravitational description.

Discussion.—Our result establishing lower and upper bounds on irreversible entropy production in holographic CFTs after quenches via the application of QNEC offers a novel perspective on the quantum thermodynamics of many-body systems.

As detailed in the Supplemental Material [44], our methods allow study of fast quenches between arbitrary *quantum equilibrium states* [74] that saturate the QNEC inequalities [Eq. (1)]. These states can be essentially described as Virasoro hair on top of vacuum and thermal states, and are dual to Banados geometries [78]. Following our methods, an erasure protocol for quantum information encoded in Virasoro hair has been implemented [79]. The QNEC inequalities reproduce the Landauer principle [80–82] and also demonstrate that certain types of encoding are tolerant against erasures faster than any microscopic timescale [79]. A more general study of transitions between quantum equilibrium states should lead to novel consequences for various quantum channels.

It is a pleasure to thank Shira Chapman, Christian Ecker, Daniel Grumiller, Arul Lakshminarayan, Prabha Mandayam, Marios Petropoulos, Giuseppe Policastro, and Suhail Ahmad Rather for helpful discussions. We also thank Souvik Banerjee for collaboration during early stages of this work, and Avik Banerjee and Nehal Mittal for collaboration on further investigations to appear in a future publication. The research of T. K. is supported by the Prime Minister's Research Fellowship (PMRF). A. M. acknowledges the support of the Ramanujan Fellowship of the Science and Engineering Board of the Department of Science and Technology of India, the new faculty seed grant of IIT Madras and the additional support from the Institute of Eminence scheme of IIT Madras funded by the Ministry of Education of India.

*Corresponding author.
tanayk@smail.iitm.ac.in
†Corresponding author.
ayan@physics.iitm.ac.in
‡Corresponding author.
pratik@physics.iitm.ac.in

[1] F. G. S. L. Brandão and G. Gour, Phys. Rev. Lett. **115**, 070503 (2015).
[2] Y. Guryanova, S. Popescu, A. J. Short, R. Silva, and P. Skrzypczyk, Nat. Commun. **7**, 12049 (2016).
[3] N. Yunger Halpern and J. M. Renes, Phys. Rev. E **93**, 022126 (2016).
[4] N. Yunger Halpern, P. Faist, J. Oppenheim, and A. Winter, Nat. Commun. **7**, 12051 (2016).
[5] J. Goold, M. Huber, A. Riera, L. d. Rio, and P. Skrzypczyk, J. Phys. A **49**, 143001 (2016).
[6] G. Gour, D. Jennings, F. Buscemi, R. Duan, and I. Marvian, Nat. Commun. **9**, 5352 (2018).
[7] E. Chitambar and G. Gour, Rev. Mod. Phys. **91**, 025001 (2019).
[8] R. Bousso, Z. Fisher, S. Leichenauer, and A. C. Wall, Phys. Rev. D **93**, 064044 (2016).
[9] R. Bousso, Z. Fisher, J. Koeller, S. Leichenauer, and A. C. Wall, Phys. Rev. D **93**, 024017 (2016).
[10] T. A. Malik and R. Lopez-Mobilia, Phys. Rev. D **101**, 066028 (2020).
[11] J. Koeller and S. Leichenauer, Phys. Rev. D **94**, 024026 (2016).
[12] S. Balakrishnan, T. Faulkner, Z. U. Khandker, and H. Wang, J. High Energy Phys. 09 (2019) 020.
[13] F. Ceyhan and T. Faulkner, Commun. Math. Phys. **377**, 999 (2020).
[14] A. C. Wall, Phys. Rev. D **85**, 024015 (2012).
[15] S. Leichenauer, A. Levine, and A. Shahbazi-Moghaddam, Phys. Rev. D **98**, 086013 (2018).
[16] N. Lashkari, J. High Energy Phys. 01 (2019) 059.
[17] M. Moosa, P. Rath, and V. P. Su, J. High Energy Phys. 01 (2021) 064.
[18] S. Deffner and E. Lutz, Phys. Rev. Lett. **105**, 170402 (2010).
[19] S. Deffner and E. Lutz, Phys. Rev. Lett. **107**, 140404 (2011).
[20] F. Plastina, A. Alecce, T. Apollaro, G. Falcone, G. Francica, F. Galve, N. Lo Gullo, and R. Zambrini, Phys. Rev. Lett. **113**, 260601 (2014).
[21] M. Angel Garcıa-March, T. Fogarty, S. Campbell, T. Busch, and M. Paternostro, New J. Phys. **18**, 103035 (2016).

[22] T. Van Vu and Y. Hasegawa, Phys. Rev. Lett. **127**, 190601 (2021).
[23] G. T. Landi and M. Paternostro, Rev. Mod. Phys. **93**, 035008 (2021).
[24] J. M. Bardeen, B. Carter, and S. W. Hawking, Commun. Math. Phys. **31**, 161 (1973).
[25] V. Balasubramanian, A. Bernamonti, J. de Boer, N. Copland, B. Craps, E. Keski-Vakkuri, B. Muller, A. Schafer, M. Shigemori, and W. Staessens, Phys. Rev. Lett. **106**, 191601 (2011).
[26] V. E. Hubeny and M. Rangamani, Adv. High Energy Phys. **2010**, 297916 (2010).
[27] P. M. Chesler and L. G. Yaffe, J. High Energy Phys. 07 (2014) 086.
[28] P. Calabrese and J. L. Cardy, J. Stat. Mech. (2004) P06002.
[29] P. Calabrese and J. L. Cardy, J. Stat. Mech. (2005) P04010.
[30] P. Calabrese and J. Cardy, J. Phys. A **42**, 504005 (2009).
[31] V. E. Hubeny, M. Rangamani, and E. Tonni, J. High Energy Phys. 05 (2013) 136.
[32] H. Liu and S. J. Suh, Phys. Rev. Lett. **112**, 011601 (2014).
[33] H. Liu and S. J. Suh, Phys. Rev. D **89**, 066012 (2014).
[34] M. Rangamani, M. Rozali, and A. Vincart-Emard, J. High Energy Phys. 04 (2016) 069.
[35] S. Leichenauer and M. Moosa, Phys. Rev. D **92**, 126004 (2015).
[36] P. Calabrese and J. Cardy, J. Stat. Mech. (2016) 064003.
[37] O. Aharony, S. S. Gubser, J. M. Maldacena, H. Ooguri, and Y. Oz, Phys. Rep. **323**, 183 (2000).
[38] J. D. Brown and M. Henneaux, Commun. Math. Phys. **104**, 207 (1986).
[39] M. Henningson and K. Skenderis, J. High Energy Phys. 07 (1998) 023.
[40] V. Balasubramanian and P. Kraus, Commun. Math. Phys. **208**, 413 (1999).
[41] K. Sfetsos, Nucl. Phys. **B436**, 721 (1995).
[42] M. Banados, C. Teitelboim, and J. Zanelli, Phys. Rev. Lett. **69**, 1849 (1992).
[43] M. Banados, M. Henneaux, C. Teitelboim, and J. Zanelli, Phys. Rev. D **48**, 1506 (1993); **88**, 069902(E) (2013).
[44] See Supplemental Material, which includes Refs. [45–47], at http://link.aps.org/supplemental/10.1103/PhysRevLett.128.191602 for general solutions describing transitions between arbitrary Banados geometries (quantum equilibrium states), details of the cut and glue method for such arbitrary transitions, analytic results for entanglement entropy and the QNEC inequalities for a final nonrotating state, more general analytic results on QNEC inequalities including dependence on the length of the entangling interval and determination of the allowed final states, and also results on the upper and lower bounds on the coefficient of the initial quadratic growth of entanglement entropy.
[45] G. Compère, P. Mao, A. Seraj, and M. M. Sheikh-Jabbari, J. High Energy Phys. 01 (2016) 080.
[46] M. M. Sheikh-Jabbari and H. Yavartanoo, Eur. Phys. J. C **76**, 493 (2016).
[47] S. Banerjee, T. Ishii, L. K. Joshi, A. Mukhopadhyay, and P. Ramadevi, J. High Energy Phys. 08 (2016) 048.
[48] S. Ryu and T. Takayanagi, Phys. Rev. Lett. **96**, 181602 (2006).
[49] V. E. Hubeny, M. Rangamani, and T. Takayanagi, J. High Energy Phys. 07 (2007) 062.
[50] This computation can be readily done by the geodetic distance formula between two end points (T_1, X_1, R_1) and (T_2, X_2, R_2) in the Poincaré patch metric. This geodetic distance L_{geo} is simply $L \ln(\xi + \sqrt{\xi^2 - 1})$, where $\xi = (Z_1^2 + Z_2^2 - (T_1 + Z_1 - T_2 - Z_2)^2 + (X_1 - X_2)^2)/2Z_1Z_2$ with $Z_{1,2} = L^2/R_{1,2}$.
[51] C. Holzhey, F. Larsen, and F. Wilczek, Nucl. Phys. **B424**, 443 (1994).
[52] M. Cadoni and M. Melis, Found. Phys. **40**, 638 (2010).
[53] R. G. Unanyan, D. Muth, and M. Fleischhauer, Phys. Rev. A **81**, 022119 (2010).
[54] R. G. Unanyan and M. Fleischhauer, Phys. Rev. A **89**, 062330 (2014).
[55] C. T. Asplund, A. Bernamonti, F. Galli, and T. Hartman, J. High Energy Phys. 09 (2015) 110.
[56] C. W. von Keyserlingk, T. Rakovszky, F. Pollmann, and S. L. Sondhi, Phys. Rev. X **8**, 021013 (2018).
[57] M. Mezei and D. Stanford, J. High Energy Phys. 05 (2017) 065.
[58] V. E. Hubeny, H. Maxfield, M. Rangamani, and E. Tonni, J. High Energy Phys. 08 (2013) 092.
[59] J. Kudler-Flam, Phys. Rev. Lett. **126**, 171603 (2021).
[60] J. Kudler-Flam, V. Narovlansky, and S. Ryu, PRX Quantum **2**, 040340 (2021).
[61] G. Mandal, R. Sinha, and N. Sorokhaibam, J. High Energy Phys. 01 (2015) 036.
[62] J. Erdmenger, D. Fernandez, M. Flory, E. Megias, A.-K. Straub, and P. Witkowski, J. High Energy Phys. 10 (2017) 034.
[63] H. Kim and D. A. Huse, Phys. Rev. Lett. **111**, 127205 (2013).
[64] G. Carleo, F. Becca, L. Sanchez-Palencia, S. Sorella, and M. Fabrizio, Phys. Rev. A **89**, 031602(R) (2014).
[65] J. Eisert, M. van den Worm, S. R. Manmana, and M. Kastner, Phys. Rev. Lett. **111**, 260401 (2013).
[66] P. Hauke and L. Tagliacozzo, Phys. Rev. Lett. **111**, 207202 (2013).
[67] G. D. Chiara, S. Montangero, P. Calabrese, and R. Fazio, J. Stat. Mech. (2006) P03001.
[68] M. Cheneau, P. Barmettler, D. Poletti, M. Endres, P. Schauß, T. Fukuhara, C. Gross, I. Bloch, C. Kollath, and S. Kuhr, Nature (London) **481**, 484 (2012).
[69] T. Langen, R. Geiger, M. Kuhnert, B. Rauer, and J. Schmiedmayer, Nat. Phys. **9**, 640 (2013).
[70] P. Jurcevic, B. P. Lanyon, P. Hauke, C. Hempel, P. Zoller, R. Blatt, and C. F. Roos, Nature (London) **511**, 202 (2014).
[71] P. Richerme, Z.-X. Gong, A. Lee, C. Senko, J. Smith, M. Foss-Feig, S. Michalakis, A. V. Gorshkov, and C. Monroe, Nature (London) **511**, 198 (2014).
[72] L. Bonnes, F. H. Essler, and A. M. Luchli, Phys. Rev. Lett. **113**, 187203 (2014).
[73] T. Hartman and J. Maldacena, J. High Energy Phys. 05 (2013) 014.
[74] C. Ecker, D. Grumiller, W. van der Schee, M. Sheikh-Jabbari, and P. Stanzer, SciPost Phys. **6**, 036 (2019).
[75] H. Casini, E. Teste, and G. Torroba, J. Phys. A **50**, 364001 (2017).
[76] J. D. Bekenstein, Phys. Rev. Lett. **46**, 623 (1981).

[77] A. Buchel, R. C. Myers, and A. van Niekerk, Phys. Rev. Lett. **111**, 201602 (2013).
[78] M. Banados, AIP Conf. Proc. **484**, 147 (1999).
[79] A. Banerjee, T. Kibe, N. Mittal, A. Mukhopadhyay, and P. Roy, arXiv:2202.00022.
[80] T. Sagawa, arXiv:1712.06858.
[81] M. Esposito, K. Lindenberg, and C. Van den Broeck, New J. Phys. **12**, 013013 (2010).
[82] D. Reeb and M. M. Wolf, New J. Phys. **16**, 103011 (2014).